Published in final edited form as:

Biosens Bioelectron. 2009 March 15; 24(7): 1843–1849. doi:10.1016/j.bios.2008.09.019.

BILAYER LIPID MEMBRANE (BLM) BASED ION SELECTIVE ELECTRODES AT THE MESO, MICRO, AND NANO SCALES

Bingwen Liu[a], **Daniel Rieck**[a], **Bernard J. Van Wie**[a,*], **Gary J. Cheng**[b], **David F. Moffett**[c], and **David A. Kidwell**[d]

[a]School of Chemical Engineering and Bioengineering, Washington State University, Pullman, WA 99164-2710

[b]School of Mechanical and Materials Engineering, Washington State University, Pullman, WA 99164-2920

[c]School of Biological Sciences, Washington State University, Pullman, WA 99164-4236

[d]Naval Research Laboratory, Washington, District of Columbia 20375

Abstract

This paper presents a novel method for making micron-sized apertures with tapered sidewalls and nano-sized apertures. Their use in bilayer lipid membrane-based ion selective electrode design is demonstrated and compared to mesoscale bilayers and traditional PVC ion selective electrodes. Micron-sized apertures are fabricated in SU-8 photoresist films and vary in diameter from 10 to 40 microns. The tapered edges in SU-8 films are desired to enhance bilayer lipid membrane (BLM) formation and are fabricated by UV-light overexposure. Nanoapertures are made in boron diffused silicon film. The membranes are used as septa to separate two potassium chloride solutions of different concentrations. Lecithin BLMs are assembled on the apertures by ejecting lipid solution. Potassium ionophore, dibenzo-18-crown-6, is incorporated into BLMs by dissolving it in the lipid solution before membrane assembly. Voltage changes with increasing potassium ion concentrations are recorded with an A/D converter. Various ionophore concentrations in BLMs are investigated. At least a 1% concentration is needed for consistent slopes. Electrode response curves are linear over the 10^{-6} to 0.1 M range with a sub-Nernstian slope of 20 mV per Log concentration change. This system shows high selectivity to potassium ions over potential interfering sodium ions. BLMs on the three different aperture sizes at the meso, micro, and nano-scales all show similar linear ranges and limits of detection (LODs) as PVC ion selective membranes.

Keywords

Ion selective electrodes; bilayer lipid membranes; microfabrication; dibenzo-18-crown-6

*Corresponding Author: Tel.: (509)335-4103; FAX: (509)335-4806, bvanwie@che.wsu.edu.

1 Introduction

Since the early work of Mueller *et al.* (1962; 1963), reconstituted bilayer lipid membranes (BLMs) have been studied by biophysicists as an ideal model for simulating complex biological membranes (Bayley and Cremer, 2001; Coronado, 1986). Recently, the application of BLMs in the design of chemical and biological sensors has been arousing increasing interest (Sugawara *et al.*, 2002; Trojanowicz and Mulchandani, 2004). BLMs are two-dimensional fluid nano structures where two phospholipids layers are joined together by non-covalent hydrophobic interaction of amphipathic molecules. They have a thickness of about 5 nm yet this varies with lipid tail length. Pure BLMs are electrically insulating and when spanning an aperture that separates two electrolyte solutions, there is generally a high resistance on the order of 100 $M\Omega \cdot cm^2$ (Tien and Ottava-Leitmannova, 2000). For analytical applications, many kinds of components such as ion channels, ion carriers, enzymes, and receptors are incorporated into lipid bilayers to endow them with functional properties (Ottava and Tien, 1997). However, the successful application of BLM based biosensors requires high stability and reproducibility, simple and flexible manufacturability, keen sensitivity, distinct selectivity, and low cost.

Traditional BLMs are reconstituted on apertures in Teflon® or other polymeric septa, separating two aqueous phases (Alvarez, 1986). The advantages of these suspended BLMs are that BLMs and solution compositions can be easily manipulated and regulated, and electrical measurements can be made from both sides of the BLMs. But the real application of traditional BLMs suffers from short-term stability on the order of minutes to hours. Thus, in order for BLMs to become the backbone in certain types of biosensors, improvement is necessary in terms of membrane longevity. Tien and Salamon reported solid-supported BLMs (s-BLM) with significantly improved longevity on the order of 36 hours, while having similar properties to suspended BLMs (Tien and Salamon, 1989). However, for ion detection, the application of s-BLMs is problematic because the solid support precludes control of the ion solution on both sides of the membrane. It is believed that the longevity of the suspended bilayers can be improved by making the holes smaller and the edges smoother (Goryll *et al.*, 2003). It is also known that the shape of the annulus plays a crucial role in the physical characteristics of the BLM (White, 1972). The annular-septum contact angle should be small for a stable arrangement. Traditionally used materials like Teflon® result in difficulties in making apertures of 100 μm or smaller, and the shape of the apertures is hard to control. However, photoresistive materials may be processed with microfabrication techniques to meet our requirements. Earlier results from our labs by Eray *et al.* (1994) showed this is possible using a polyimide structure; results showed a smooth 30 μm aperture with a sharp taper angle capable of supporting bilayers that house the nicotinic acetylcholine ion channel. However, the sensing approach in this early work requires sophisticated and expensive patch clamp equipment to measure pico-ampere currents from individual ion channels and therefore has limitations for practical sensing applications. Similar sensors introduced by others rely on conductance (Rebak te al., 1993), current (Wu *et al.* 2000), fluorescence (Worsfold *et al.*, 2004), capacitance measurements (Cheng *et al.*, 2001), and single-channel responses (Hirano *et al.*, 2003; Nozawa *et al.*, 2007) resulting from the change of the electrical and structural properties of BLMs to detect analyte concentrations.

However, a more attractive and practical approach is to use BLMs and lipophilic ionophores along with simple portable electronics packages available for measuring voltages in ion selective electrodes (ISEs) (Minami *et al.*, 1991; Sato *et al.*, 1997).

In this work, we introduce a novel design in which tapered micro-fabricated apertures in the photoresist SU-8 serve as supports for BLMs. Fabrication techniques for apertures of the various sizes from the micro- to the nano- scales are presented. Excellent mechanical strength with a Young's Modulus of 4.0 ~ 4.9 GPa, low dielectric constant with values of 3 ~ 4, and a hydrophobic surface make SU-8 a desirable material for supporting BLMs. Dibenzo-18-crown-6 is used as the ionophore for the potassium ion. We assess this system for its potential in forming self assembled bilayer ISEs and compare results to polymer-based ISEs and BLMs formed on the typical sub-millimeter Teflon® aperture BLM chambers. We show good to excellent agreement in response range, limits of detection (LODs), and interferences from the common Na^+ ions. Finally, preliminary results from BLMs formed on nano-apertures made from boron–doped silicon films are presented and compare well to BLMs made on the large apertures.

2 Materials and Methods

2.1 Materials and Equipment

Silicon wafers are of the P-type, 3" in diameter, <100> orientation, 1–100 ohm·cm, with a thickness of 380 μm from University Wafer Inc. (South Boston, MA). SU-8 (MicroChem Corp., Newton, MA) is used as the negative photoresist and AZ5214 (Clariant Corporation, Somerville, NJ) as the positive photoresist. The photo mask consisting of transparent plastic film used for printing transparencies is made from University Publishing at Washington State University (WSU) (Pullman WA), and has 20, 30, 60, 80 and 100 μm black dots printed on it. Photolithography is performed using the contact method in a Model 500 mask aligner (Optical Associates Inc., San Jose, CA). Supplemental Files in the electronic version of the manuscript contain details on test chambers, BLM and PVC ISE formation, signal recording, and Na^+ control experimental aspects of the work.

2.2 Micro-aperture Chip Fabrication Procedure

A schematic of the microscale fabrication procedure is shown in Figure 1. System construction begins with spin coating of photoresist AZ5214 onto a silicon wafer (a) which serves as a support base during construction. This photoresist layer serves as a sacrificial layer to later separate the silicon wafer from the SU-8; it is spin coated with SU-8 at 3000 RPM (b) to create a 10 μm-thick SU-8 layer. The sample is covered with an appropriate photomask and exposed to UV light (c). For the photo mask we use 32 1 cm × 1 cm squares in the middle of which are black dots of various sizes. Exposure times from 3 to 15 minutes are used. This is longer than the 18 seconds recommended by Micro Chem Corporation and results in scattering of light underneath the mask dots to expose this area. Less light is scattered near the surface with an ever increasing amount of scatter as light proceeds vertically downward – during the developing process the pattern leads to the desired tapered and sharp-edged apertures. The sample is then developed with SU-8 developer (d). Because SU-8 is a negative photoresist, the exposed area of SU-8 is hardened. However, chemical

bonds in the positive photoresist AZ5214 are weakened, except for directly underneath the masked area. A ring of superglue (Loctite, Rocky Hill, CT) is dispensed onto a 4 mm diameter window in the center of thin 1 cm^2 plastic chips (e) cut from the plastic material from the bottom of Petri dishes; the thin film of patterned SU-8 is then carefully placed onto the plastic chip making sure the micropore area is maintained in the center of the window. After the glue is hardened, the wafer is dipped into AZ400K developer to etch away the AZ5214 exposed to UV light through the transparent SU-8 layer; the non-exposed AZ5214 is detached because it is directly under the hole left by the negative photoresist process. This serves to completely remove the silicon substrate (f).

2.3 Nanoaperture Chip Fabrication Procedure

The fabrication procedure for nanoscale apertures is shown in Figure 2. The fabrication starts with a bare silicon wafer which is oxidized at a temperature of 1000 °C for 90 min, so that a silicon dioxide layer covers the wafer (a). While we protect one side of the wafer by attaching tape (Semiconductor Equipment Corp., Moorpark, CA), silicon dioxide on the other side is etched away by buffered oxide etch (Bras *et al.*, 2004) (b). Boron is diffused into the exposed silicon surface for 110 min to create a 2-μm thick boron diffused silicon layer (c), which is used as an etch stop in a later step to provide a thin membrane in which the aperture will be made. An oxidation step at 850 °C for 60 min (d) creates a silicon dioxide layer on the both sides of the wafer which is then etched away (e) to remove impurities, i.e. a boron skin (An *et al.*, 1983), developed during boron diffusion, leaving behind a wafer with a boron diffusion layer. The wafer is oxidized again at a temperature of 850 °C for 150 min (f). A gold layer of approximately 500 nm thickness is sputtered on the non-boron side of the wafer (g) to protect the non-patterned silicon while etching through the wafer. Annealing at 700 °C for 10 min results in effective adhesion between layers. The gold and silicon dioxide layers are then patterned by photolithography (h). Then the wafer is clamped in a special homemade carrier and put into KOH etchant consisting of 300 g KOH, 600 mL dH_2O and 120 mL isopropyl alcohol. The etching stops at the boron diffused layer, leaving a thin 2-μm thick membrane (i). At this point the gold layer has served its purpose and is removed by gold etching solution (Mura *et al.*, 2003) (j). Polymethyl methacrylate (PMMA) is spin coated on the chip and patterned by E-beam lithography. A nanoscale hole is drilled through the membrane with reactive ion etching (k). The silicon chip is oxidized at 800 °C for 2 hours to create an electrically insulting covering on the nanoaperture. Liquid phase hexamethyldisilizane (HMDS) is applied to make the surface of the apertures hydrophobic to attract the lipid tails of the phospholipids that comprise the bilayers.

3 Results and Discussion

3.1 Micro Apertures

Figure 3 shows the various apertures manufactured in this study. Figure parts 3a – 3c represent those fabricated in SU-8 film with diameters of about 10 and 40 μm with the tapered shape created by diffraction of the UV light in fabrication steps. Therefore, exposure time to UV light is critical. The smallest diameter obtained with this design is on the order of 10 μm and is prepared using 20 ~ 30 μm mask dots. Required exposure time varies with the sizes of mask dots. Too long of exposure leads to excessive crosslinking of the SU-8

substrate and disappearance of the aperture structure as shown in Figure 3 (c). The optimal procedure found for 20 to 30 μm dots is to use a 3 ~ 4 min exposure time resulting in 10 μm holes. For 80 or 100 μm dots an optimal 10 ~ 15 min exposure time exists that results in 30 ~ 40 μm holes with excellent taper characteristics; given the favorable tapered geometry these apertures are well suited for use in our BLM studies and selected for further experimentation. Though the 60 μm dots were not tested in this set of studies we predict that holes of intermediate size will result on the order of 20 ~ 30 μm when 8 ~ 10 min exposure times are used.

3.2 Nanoapertures

An etched pyramid-shaped window with a thin silicon membrane at the bottom is created by anisotropic wet etching of KOH toward the <100> orientation silicon wafer along (111) crystal planes at an etching rate of 1 μm/min at 80°C. Figure 3(d) shows a SEM picture of a nanoaperture which is on the order of 660 nm in diameter. An aperture with roughly vertical side walls is produced because the charged ions bombard only the normal surface of the substrate during reactive ion etching.

3.3 BLM Ion Selective Electrode Response, BLM Confirmation and Stability

Figure 4 shows K^+ calibration curves for dibenzo-18-crown-6 BLMs in our 40 μm SU-8 micro apertures and for 660 nm silicon apertures compared to a set of controls. Table 1 shows a comparison of response slopes, linear ranges and LODs for these BLMs compared to those formed in meso-sized 350 μm apertures and a standard K^+ ISEs made in PVC-plasticizer membranes. Collective inspection of all the values reported reveals tight standard deviations that substantiate the validity of the data. LODs are calculated by the intersection of a line parallel to the x-axis through the mean of the potential values measured at the lower concentrations and the best fit slope in the linear region of the calibration curve. All methods result in K^+ electrodes that display the typical character of ISEs with positive slopes, a linear range over several orders of magnitude and response times on the order of 9 ~ 20 sec (determined as the time it takes to reach 90% of the final average value). The 9 sec time for the PVC ISE is consistent with the 5 – 10 sec response times typically observed for PVC ISEs in our laboratory while the BLMs have average response times that are nearly double the PVC value (85% higher). The micron, nanometer and PVC ISEs all have good LODs on the order of $10^{-5.3}$ or lower and good linear responses in the range of $10^{-5} \sim 10^{-0.3}$; the 350 μm aperture shows slightly less desirable values of a $10^{-4.6}$ LOD and a $10^{-4.2} \sim 10^{-0.3}$ linear range. Concerning the response slopes, however, only the PVC ISE has the typical near Nernstian 50 or more mV/Log[C] response slope observed in our lab for monovalent cations (Plesha *et al.*, 2006). The slope for the 350 μm BLM ISE is 35.1 mV/Log[C] or 79% of the PVC ISE value while those for the increasingly smaller 40 μm SU-8 and 660 nm silicon apertures show diminishing slopes of 20.1 and 15.8 mV/Log[C] which are 45% & 36% of the PVC response, respectively. As this is the first instance in which BLMs are made on the SU-8 and silicon structure these results are encouraging. Similarly the nanoapertures show success in providing an electrically insulating layer through surface oxidation of the silicon that by itself is semi-conductive, and success in converting the hydrophilic SiO_2 surface to a hydrophobic surface that can support BLMs.

As already stated what is truly important in this paper is the presentation of voltage responses in BLMs formed on micro- and nanoapertures. However, one must also confirm that these types of structures truly contain bilayers and that they are at least reasonably stable. Supporting evidence for BLM formation is provided in micro-aperture preparations where we observe a gramicidin induced current change by one order of magnitude from ~10 to ~150 pA after membrane formation similar to that reported (Montal and Mueller, 1972). Also, these membranes show the characteristic increase in capacitance (Tien 1974) that occurs with membrane thinning on bilayer formation with increases up to 0.42 μF/cm^2. Concerning stability BLMs were shown to be stable up to tens of hours which is consistent with our previous findings when using polyimide structures (Eray *et al.* 1994).

It is also important to consider some possible explanations of the non-Nerstian behavior and the small positive responses in control studies. Such explanations add insight for the future refinement in fabrication procedures that potentially will provide improved responses. For example, one explanation for the smaller slopes for the BLMs can be understood by assessing the impact of the thin ring of lipid around the annular circumference that has not formed a bilayer (Nikolelis *et al.*, 1996). Such rings are commonly found in BLMs and consist of lipids of amorphous orientation. Although a whole phophatidylcholine molecule is neutral, its non-uniform charge distribution, positive charge exposure to aqueous solution and high orderly arrangement in bilayers can induce local surface charges in aqueous solution close to the bilayer surfaces. Ion exchange with the surrounding aqueous phase would give a small conductivity through the amorphous structure. Data from the control study for the K^+ response without ionophores supports this hypothesis as a slight positive potential for K^+ appears after the 0.01 M concentration with a potential of +20 mV in the 0.6 M K^+ range. Further support is offered by the fact that the tapered micro apertures and thin nanoapertures have LODs and linear ranges an order of magnitude lower than the 350 μm Teflon aperture. The tapered structures are less likely to have thick annular rings and this further supports the necessity of using fabrication techniques that employ optical diffraction of light underneath a mask to obtain the tapered shape. Future optimization studies on taper angles and the corresponding BLM ISE behavior will be helpful in this regard.

3.4 Effects of Ionophore Concentrations on Membrane Potentials

The effect of the ionophore concentrations on the response to K^+ is also found to be important. In these experiments the lipid solutions with ionophores in them must be prepared by taking into account the approximate residual amount of solvent. As determined in the work of White (1976) and Blumenthal *et al.* (1982), about 30% the original solvent is assumed to remain in a bilayer; this finding is used in establishing the resultant amount of ionophore in a given membrane. As shown in Table 1 and Figure 5 the concentration of ionophore plays an important role in ISE response character. First of all, however, we note the similar fast responses in the range of 14 to 20 seconds as exhibited in our first study on the various ISE platforms. It is instructive to note however that the 0.1 and 0.5% ionophore concentrations result in response times 33% higher than the collective average responses for the higher percentage ionophores. Also, the ISE response slope of the 0.1% ionophore membrane is a mere 35% of the value for the collective average values for the 1, 4 and 8% ionophore ISEs while the 0.5% ionophore composition gives a slope that is 90% of this

average. LODs and lower end concentration of the linear response ranges are two orders of magnitude higher in concentration for the 0.1% and the 0.5% ionophore levels than the collective average for the 1, 4 and 8% ionophore ISEs.

From an initial assessment of the situation one might attribute the differences to the reduced rate of transport of charges across the membrane when ionophore concentrations fall below 1%. This would account for the longer response time. However, one could incorrectly conclude that the reduced molecule number of ionophore is insufficient to maintain the Nernst equilibrium across the BLM. This is because an ISE, is a battery, and has an open transmembrane potential dependent on the concentrations of transmembrane ions, relative selectivities and a parameter to account for what we refer to as an unknown interference coefficient as modeled by a modified Nikolsky-Eisenman equation (Plesha *et al.* 2006). Therefore an ISE voltage is not dependent on the concentration of the ionophore and we would expect, since none of model values change at a given K^+ concentration, no change in voltage with ionophore concentration. However, this is theory – not reality. The voltage we are talking about is the open circuit voltage – the voltage where no current (power) is being drawn from the cell. Once one makes a measurement, current (power) is drawn to make that measurement. If the current carriers, i.e. the ionophores are low in concentration, then the voltage drops because the number of carriers in the membrane account for the resistance to charge movement. This is supported by the early work of Keating and Rechnitz (1984) who report transmembrane voltage modulation with antibody trapping of ionophore to one side of the membrane. This results in a higher resistance to current flow due to reduced facilitated transport of K^+. Yet, the important conclusion of this study is, given the equipment used for making measurements and the nature of the responses, a 1% level of ionophore concentration is sufficient to circumvent diminishing responses and no advantage is gained by using higher concentrations of ionophores as the response times, slopes, LODs, and linear ranges are in good agreement for these higher concentrations.

4 Conclusions

New fabrication techniques are presented for making BLM supporting apertures in SU-8 films and silicon wafers. Though the manufacture of nano and micro-apertures is more complex compared to traditional methods used to make meso-scale pores, the new techniques offer alternative support structures that will allow miniaturization of bilayers-based sensors. Such supports also will likely improve membrane stability and such studies are under investigation. For SU-8 various sized apertures in the 10 to 40 μm range are obtained by using a photomask with a series of mask dot diameters. To obtain the desired tapered shape of the aperture edge, a UV light overexposure technique is used which causes diffraction of the light to regions directly underneath the mask dots. Optimal exposure times vary as a function of the mask diameter with too long of an exposure resulting in a complete undercutting of the negative SU-8 photoresist and prevention of aperture formation. For silicon nanoapertures e-beam lithography and reactive ion etching are successful in fabricating 660 nm apertures while surface oxidation and HMDS coating result in an electrically insulting and hydrophobic structure which can support BLM ISEs.

The sensing is based on the voltage variations across bilayers that can be easily measured. A set of experiments show LODs and linear ranges with similar values for PVC ISEs, and the BLM ISEs on the 40 μm SU-8 chips and 660 nm silicon chips. On the other hand response times are nearly double for the micro- and nanoscale BLMs, and BLM slopes are sub-Nernstian with a value for the best electrode that is 50% of the PVC response slope. Presumably the lower slope is attributable to a lipid annulus around the lip of the apertures that is able to conduct ions. Nevertheless, sensing may be accomplished adequately using the BLM ISEs. Besides the self-assembly properties of lipids, an advantage over standard polymer ISEs is that the dibenzo-18-crown-6 BLMs appear to have no selectivity for Na^+, though further research may reveal this is due to co-conductivity of Cl^- ions due to charged groups in the amorphous annular ring around the lip of the apertures.

It is also found that ionophore concentrations in BLMs have a critical effect on membrane potential. When the concentration of ionophore is significantly less than 1%, sensors become less sensitive to K^+ with a 0.5% ionophore BLM showing a reduction in slope by 10% and a 0.1% ionophore by a 65% reduction. Response times are also 33% higher for these ISEs. At the same time the lower ionophore concentrations result in LODs that are two concentration logs below those for the concentrations of 1% or above. This also has a dramatic impact on the linear range reducing it by one to two orders of magnitude. A reasonable explanation seems to be offered by considering the impact of higher membrane resistances, due to the lower concentration of carrier species, on the actual measurement of the membrane potential. However, when the ionophore concentration is greater than 1% it appears diffusion limitations are overcome and no further increase in performance is observed.

Supplementary Material

Refer to Web version on PubMed Central for supplementary material.

Acknowledgements

We acknowledge research support from the National Science Foundation Grant BES BES-0508521, the NIH biotechnology Training Grant NIH 5T32-GM008336-16, the Technical Support Working Group Contract T-242A and the Washington State University School of Chemical Engineering and Bioengineering.

References

Alvarez, O. Ion Channel Reconstitution. Miller, C., editor. New York: Plenum; 1986. p. P115-P130.

An DK, Mai LH, Hoi P. Physica Status Solidi (a). 1983; 76(1):K85–K88.

Bayley H, Cremer PS. Nature. 2001; 413(6852):226–230. [PubMed: 11557992]

Blumenthal, R.; Klausner, KD. Membrane Reconstitution. Poste, G.; Nicolson, GL., editors. Amsterdam: North-Holland Pub. Co.; 2001. p. P45

Bras M, Dugas V, Bessueille F, Cloarec JP, Martin JR, Cabrera M, Chauvet JP, Souteyrand E, Garrigues M. Biosensors & Bioelectronics. 2004; 20(4):797–806. [PubMed: 15522595]

Cheng Z, Luo L, Wu Z, Wang E, Yang X. Electroanalysis. 2001; 13(1):68–71.

Coronado R. Annual Review of Biophysics and Biophysical Chemistry. 1986; 15:259–277.

Eray M, Dogan NS, Liu L, Koch AR, Moffett DF, Siber M, Van Wie BJ. Biosensors & Bioelectronics. 1994; 9(4–5):343–351.

Goryll M, Wilk S, Laws GM, Thornton, Goodnick TS, Saraniti M, Tang J, Eisenberg RS. Superlattices and Microstructures. 2003; 34(3–6):451–457.

Hirano A, Wakabayashi M, Matsuno Y, Sugawara M. Biosensors and Bioelectronics. 2003; 18(7):973–983. [PubMed: 12782460]

Keating MY, Rechnitz GA. Analytical Chemistry. 1984; 56(4):801–806. [PubMed: 6721153]

Minami H, Sato N, Sugawara M, Umezawa Y. Analytical Science. 1991; 7(6):853–862.

Montal M, Mueller P. Proceedings of the National Academy of Science. 1972; 19(12):3561–3566.

Mueller P, Rudin DO, Tien HT, Wescott WC. Nature. 1962; 194(4832):979–980. [PubMed: 14476933]

Mueller P, Rudin DO, Tien HT, Wescott WC. Journal of Physical Chemistry. 1963; 67(2):534–535.

Mura G, Vanzi M, Stangoni M, Ciappa M, Fichtner W. Microelectronics Reliability. 2003; 43(9):1771–1776.

Nikolelis DP, Siontorou CG, Krull UJ, Katrivanos PL. Analytical Chemistry. 1996; 68(10):1735–1741. [PubMed: 8651482]

Nozawa K, Osono C, Sugawara M. Sensors and Actuators B. 2007; 126(2):632–640.

Ottava AL, Tien HT. Bioelectrochemistry and Bioenergetics. 1997; 42(2):141–152.

Plesha MA, Van Wie BJ, Mullin JK, Kidwell DA. Analytica Chimica Acta. 2006; 570(2):186–194. [PubMed: 17723398]

Rebak M, Snejdarkova M, Otta M. Electroanalysis. 1993; 5(8):691–694.

Sato H, Wakabayashi M, Ito T, Sugawara M, Umezawa Y. Analytical Science. 1997; 13(3):437–446.

Sugawara M, Hirano A, Bühlmann P, Umezawa Y. Bulletin of the Chemical Society of Japan. 2002; 75(2):187–201.

Tien, HT. Bilayer Lipid Membranes (BLM): Theory and Practice. New York: Marcel Dekker Inc.; 1974. p. P137

Tien, HT.; Ottava-Leitmannova, A. Membrane Biophysics. Netherlands: Elsevier, Amsterdam; 2000. p. P168

Tien HT, Salamon Z. Bioelectrochemistry and Bioenergetics. 1989; 22(3):211–218.

Trojanowicz M, Mulchandani A. Analytical and Bioanalytical Chemistry. 2004; 379(3):347–350. [PubMed: 15085317]

White SH. Biophysical Journal. 1972; 12(4):432–445. [PubMed: 5019479]

White SH. Nature. 1976; 262(5567):421–422. [PubMed: 958398]

Worsfold O, Toma C, Nishiya T. Biosensors & Bioelectronics. 2004; 19(11):1505–1511. [PubMed: 15093223]

Wu Z, Wang B, Dong S, Wang E. Biosensors & Bioelectronics. 2000; 15(3–4):143–147. [PubMed: 11286331]

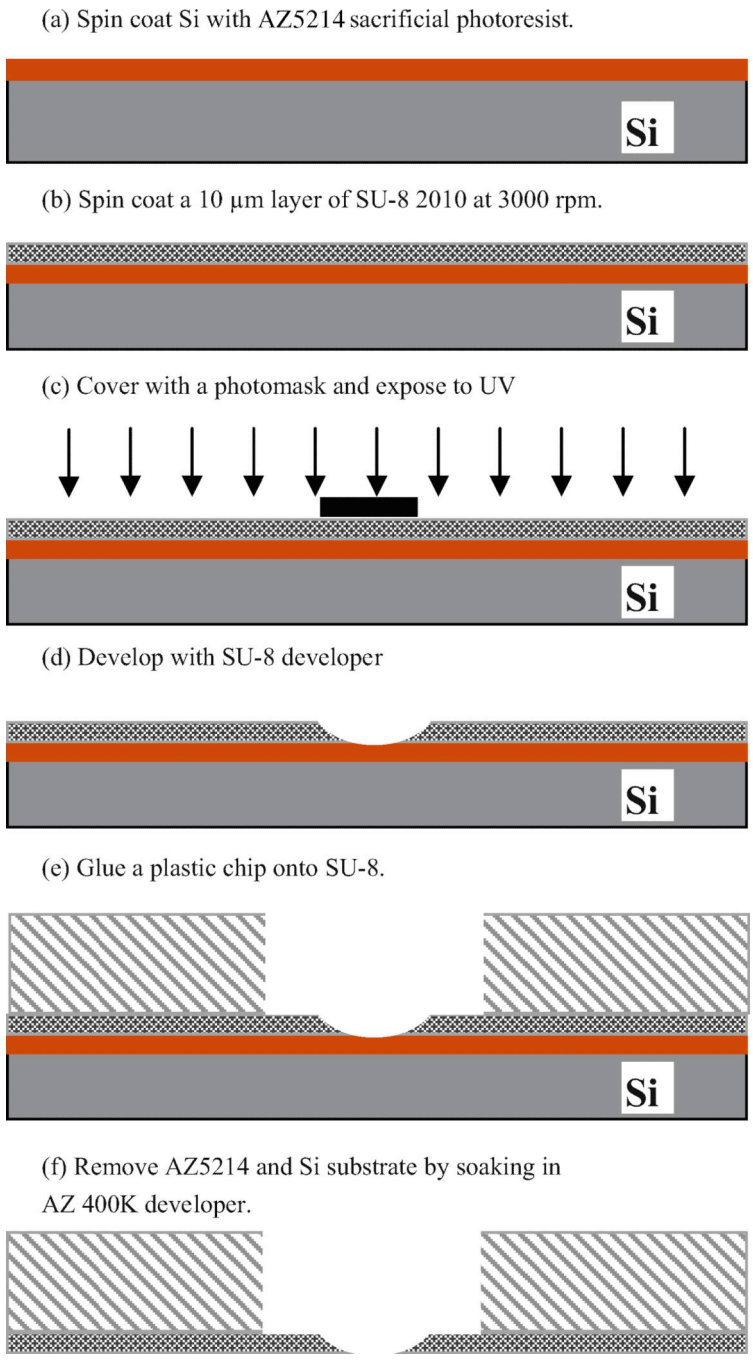

Figure 1.
SU-8 aperture micro-fabrication procedure and mounting onto plastic chips.

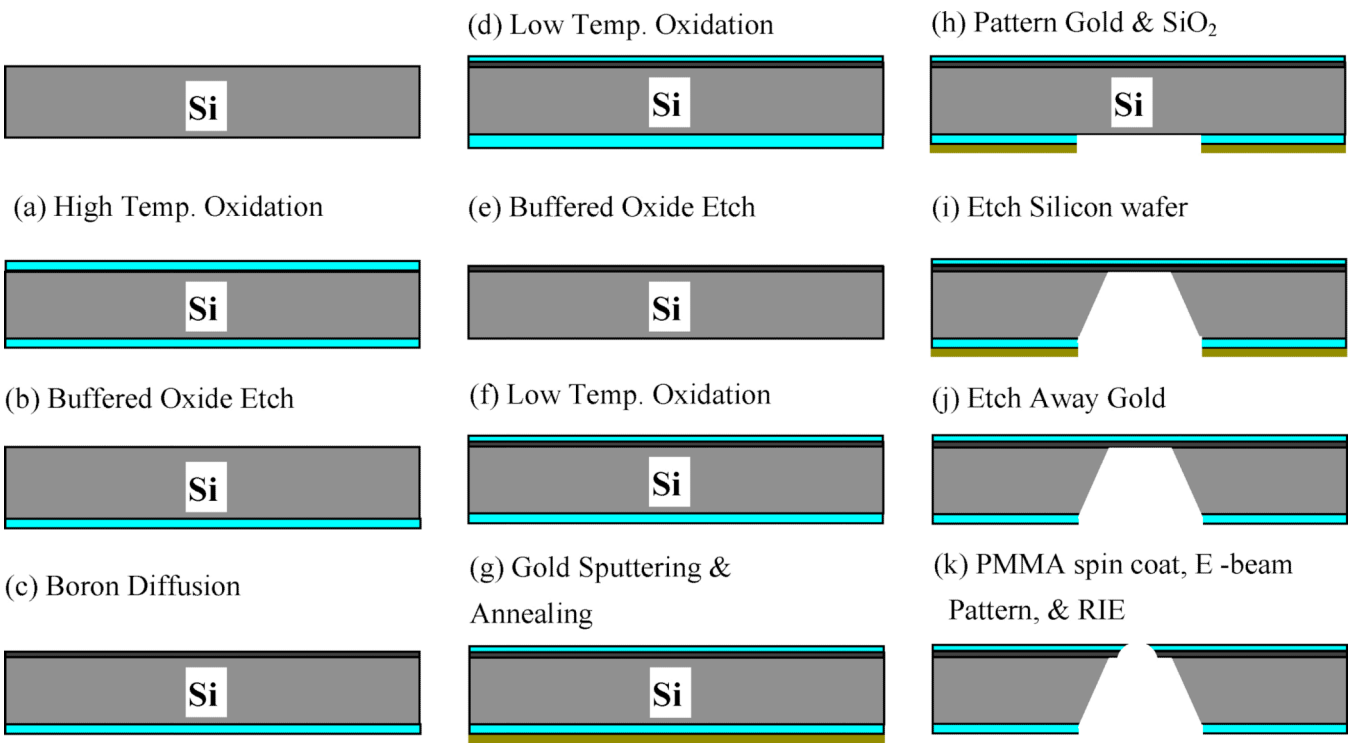

Figure 2.
Nanoaperture chip fabrication procedure.

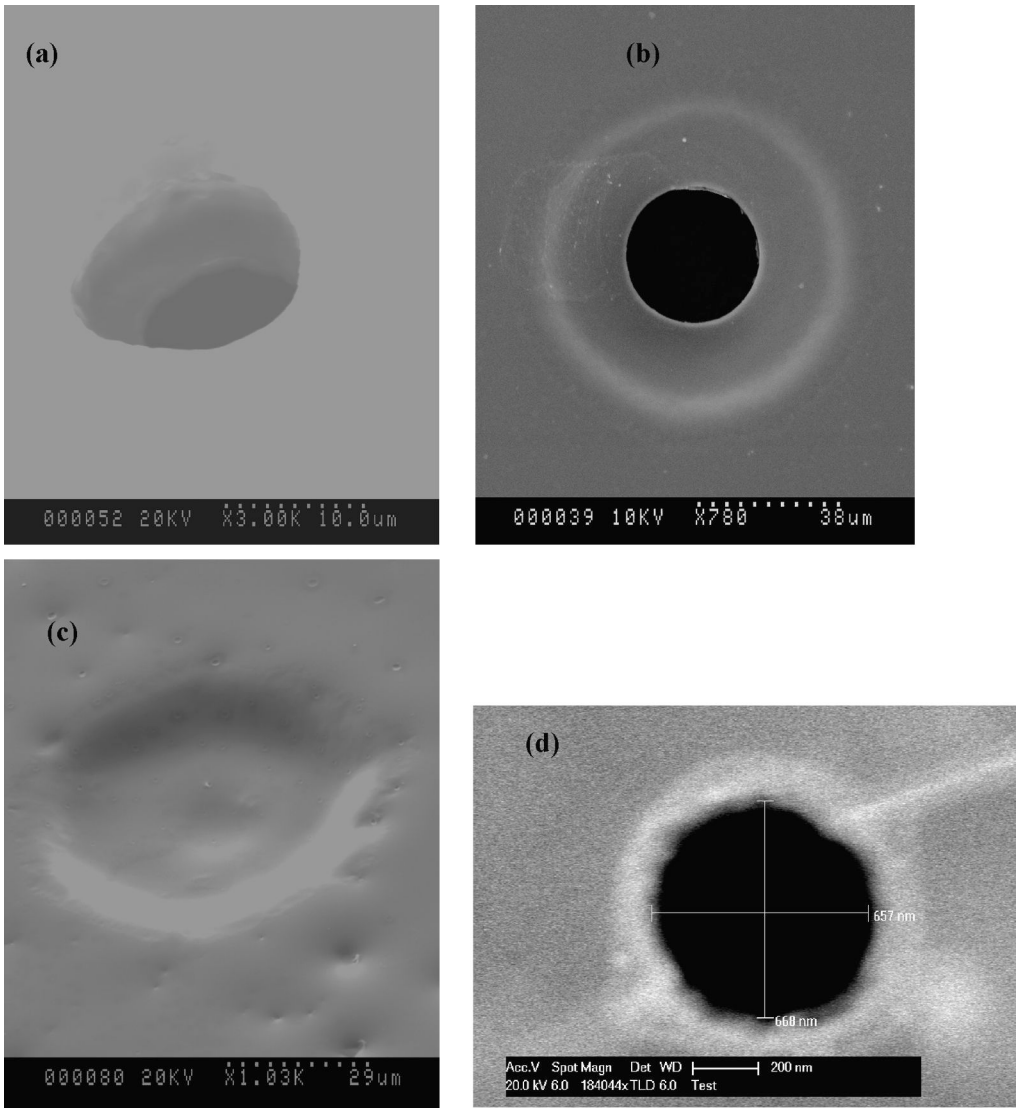

Figure 3.

SEM pictures of apertures in SU-8 film and nano-aperture. (a) A 10 μm aperture, the smallest diameter that can be made with the approach presented; (b) show a SU-8 aperture of about 40 μm; (c) Fabrication failure due to over exposure to UV light; (d) an silicon aperture of about 660 nm.

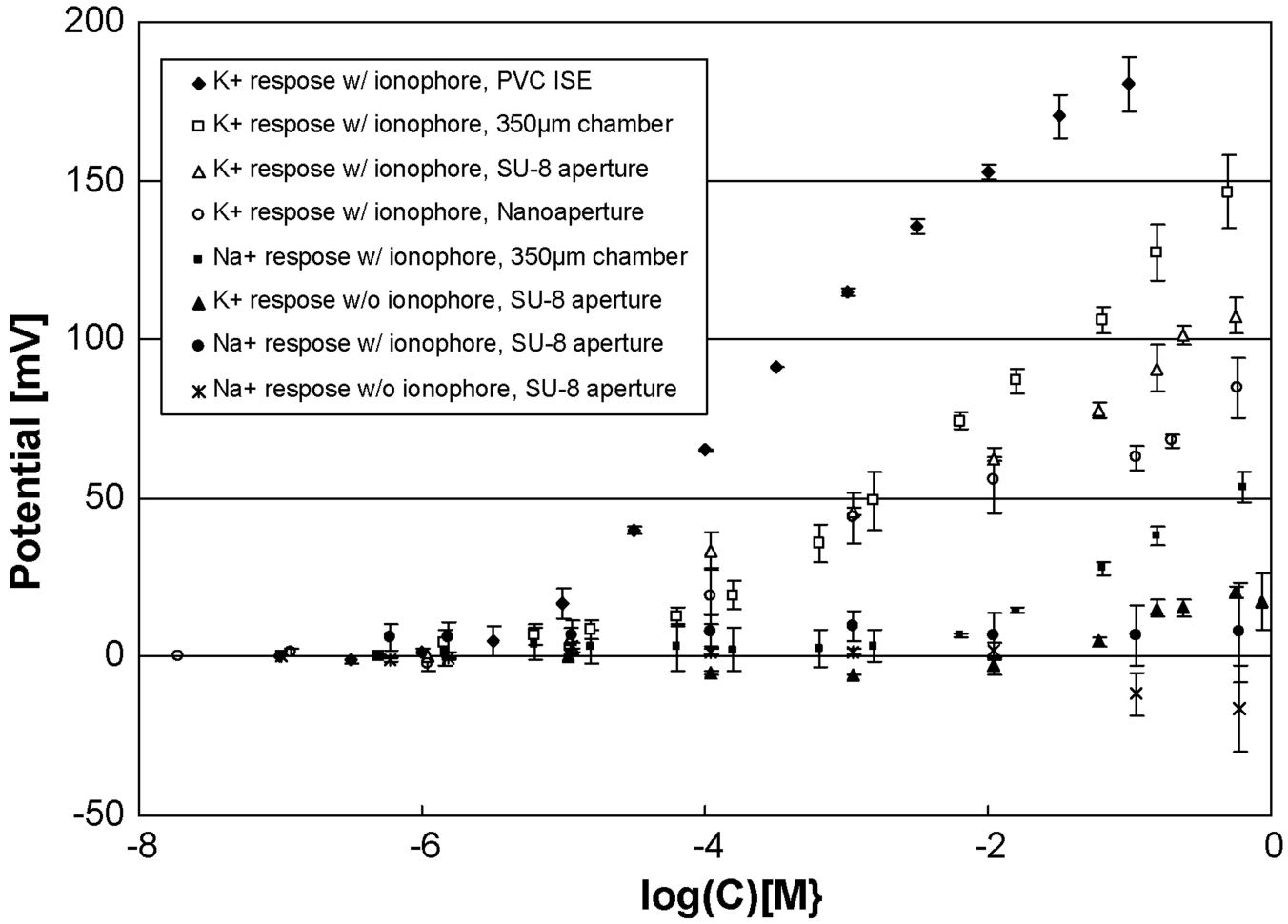

Figure 4.

Calibration curves for K^+ compared with control curves without ionophores and for Na^+. The dibenzo-18-crown-6 ionophore shows flexibility in its use as an ionophore in PVC and lipid bilayers with good linear response ranges, LODs on the order of 10^{-5}, high selectivity for K^+ over Na^+ and slopes that are near Nernstian for the PVC and 47% of the PVC value for the SU-8 and 32% of the value for the silicon nanoaperture. SU-8 results are with the 40 µm apertures, while the silicon nanoaperture is 660 nm in size, and the conventional chamber a 350 µm Teflon® aperture.

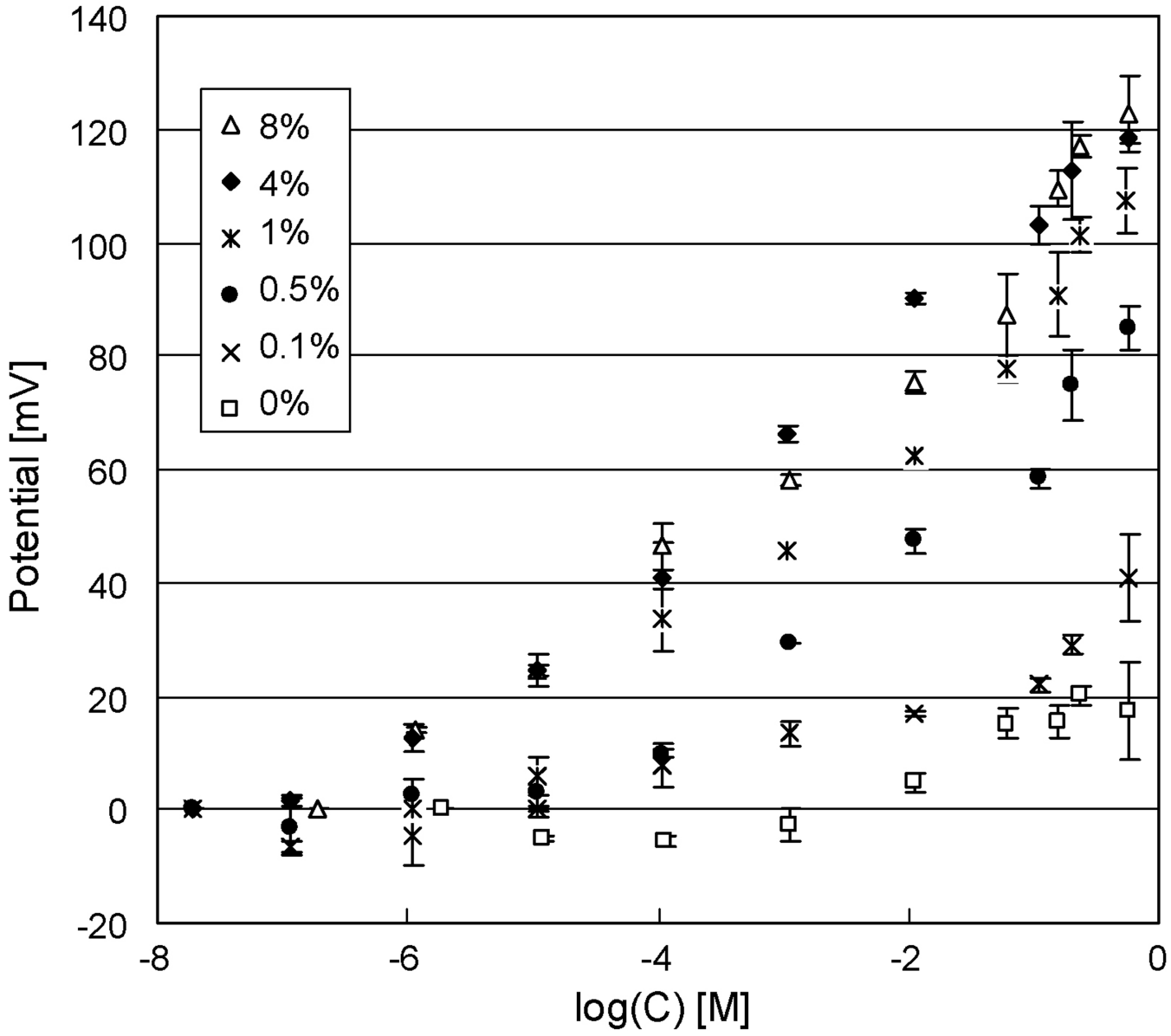

Figure 5.

The effects of ionophore concentrations on electrode responses. Increasing concentration of dizenzo-18-crown-6 from zero to 1% results in increasing membrane potentials. When the concentration of debenzo-18-crown-6 is above 1% membrane potentials are no longer affected by the amount of ionophores in the membrane.

Table 1

Summary of electrode performance and comparison with PVC ISEs.

Experiment	Electrode type	Slope [mV/log]	Linear Range [log(K^+)]	LOD [log(K^+)]	Response Time [sec]
Comparison	PVC ISE	44.4±1.8	−5.5 ±0.1~ −1.3±0.3	−5.5±0.1	9±1.2
of Standard PVC ISE	350μm Teflon® aperture	35.1±4.4	−4.5±0.3 ~ −0.3±0.1	−4.4±0.3	16±1.5
to BLM	40 μm SU-8 aperture	20.1±0.6	−5.0±0.1 ~ −0.3±0.1	−5.3±0.1	14±3
ISEs	660 nm silicon aperture	15.8±0.1	−5.5±0.5 ~ −0.2±0.1	−5.3±0.3	20±3.4
	0.1% ionophore	7.00±0.1	−5.0±1.0 ~−0.5±0.3	−4.7±0.3	20±5.1
Comparison of	0.5% ionophore	18.8±1.7	−4.5±0.5 ~ −0.3±0.1	−4.5±0.2	20±4.7
BLM Ionophore	1.0% ionophore	20.1±0.6	−5.0±0.1 ~ −0.3±0.1	−5.3±0.1	14±3
Concentrations[(a)]	4.0% ionophore	18.9±0.9	−6.5±0.5 ~ −0.2±0.1	−6.5±0.1	15±2.7
	8.0% ionophore	19.1±1.1	−5.5±0.5 ~ −0.2±0.1	−6.2±0.2	16±2.5

[(a)] With a SU-8 aperture of 40 μm in diameter.